PHYSICAL REVIEW B **96**, 060505(R) (2017)

Majorana zero modes in a two-dimensional *p*-wave superconductor

Võ Tiến Phong,[1,*] Niels R. Walet,[1,†] and Francisco Guinea[1,2,‡]
[1]*School of Physics and Astronomy, University of Manchester, Manchester, M13 9PY, United Kingdom*
[2]*Imdea Nanoscience, Faraday 9, 28015 Madrid, Spain*

(Received 3 February 2017; revised manuscript received 31 July 2017; published 15 August 2017)

We analyze the formation of Majorana zero modes at the edge of a two-dimensional topological superconductor. In particular, we study a time-reversal-invariant triplet phase that is likely to exist in doped Bi_2Se_3. Upon the introduction of an in-plane magnetic field to the superconductor, a gap is opened in the surface modes, which induces localized Majorana modes. The position of these modes can be simply manipulated by changing the orientation of the applied field, yielding novel methods for braiding these states with possible applications to topological quantum computation.

DOI: 10.1103/PhysRevB.96.060505

Topological quantum computation is currently among the most interesting candidates for the realization of a universal quantum computer [1]. This approach provides a promising path to creating a robust qubit that can endure the necessary manipulations required in performing quantum logic [2]. Recent attempts at realizing such a qubit in condensed-matter platforms are motivated by the one-dimensional Kitaev model [3] with a topological insulating wire on which superconductivity is induced by contact with an ordinary *s*-wave superconductor [4,5]. Systems of such qubits are presently the subject of many investigations; see, for example, Ref. [1] and references contained therein.

Many approaches to topological quantum computation are based on the creation and manipulation of massless Majorana states [3]. These arise as excitations in a two-dimensional system when a fermion is effectively split into two parts, with each part localized far away from the other in space. Since fermions are fundamental particles, Majorana states are always generated in pairs. Such states are known to occur in topological superconductors [6–13] and have been predicted to exist in the $\nu = \frac{5}{2}$ fractional quantum Hall effect [14,15]. Because of their nontrivial half-fermion statistics, braiding, or exchanging, Majorana states is a non-Abelian process which takes place within the space of degenerate ground states. Quantum gates can be built by simply braiding Majorana states [8]. Currently, realistic schemes for braiding Majorana states require triwire junctions [16], and either electrostatic gates [17] or controllable magnetic fluxes [18].

In this Rapid Communication, we propose and study a solid-state platform for the creation and manipulation of Majorana states, motivated by current research on natural topological superconductors. Our proposed system is modeled on doped Bi_2Se_3, but the results we present here are more general, and can be extended to other superconductors and to the superfluid *B* phase of ^{3}He. In what follows, we describe the general features of the Majorana platform, and show by detailed calculations how these Majorana states arise. We then discuss a simple scheme for manipulating Majorana excitations on superconducting disks. Using a simple extension, we show that one can study our model in arbitrary geometries, providing further impetus for experimental realization. This is described in full detail in the Supplemental Material [19].

We start with a thin disk of a topological superconductor material with thickness smaller than the superconducting coherence length, as sketched in Fig. 1. In this limit, the surface states at the top and bottom surfaces hybridize and develop a small gap. The only remaining subgap states are quasi-one-dimensional gapless Majorana bands localized at the edges. If time-reversal symmetry (TRS) is not broken in the superconducting phase, there are two bands related by TRS inside the gap. An in-plane magnetic field applied to the system, as shown in Fig. 1, breaks time-reversal symmetry. This field hybridizes the two sets of Andreev states, and opens a gap in the energy spectrum. The sign and magnitude of the gap are determined by the normal of the field to the edge and is opposite where the field enters the disk to where the field exits the system. This leads to the formation of Majorana modes located inside the bulk energy gap. These Majorana edge modes are localized near the boundary of the disk, at the points where the field is parallel to the edge.

Of the different order parameters that have been proposed to describe the superconducting phase of doped Bi_2Se_3 [20–22], we will consider a time-reversal-invariant, odd-parity, triplet phase. Our analysis applies to similar Majorana modes appearing in neutral fermionic superfluids, such as ^{3}He [23–25] (see also [26]), as well as to gapped atomic Fermi superfluids [27]. In general, the two requirements for our proposed system are (i) (effective) two-dimensionality, and (ii) existence of gapless counterpropagating Andreev edge modes. The first condition requires the thickness of the system to be smaller than the superconducting coherence length. The second condition excludes a two-dimensional, gapped chiral $p_x \pm ip_y$ superconductor, as the corresponding edge modes flow in one direction only. Our results can be generalized to other topological superconducting phases, provided that the gap does not vanish on the Fermi surface, in particular to two-component time-reversal-invariant nematic phases [21,22]. Related artificial topological superconductors can be created using the proximity effect [28–30].

We describe the system using a two-orbital, $\mathbf{k}\cdot\mathbf{p}$ Hamiltonian proposed for the topological insulator Bi_2Se_3 [31–33]. We consider quasi-two-dimensional systems, of thickness d such that $k_{Fz}^{-1} \ll d \lesssim \xi_z$, where k_{Fz} and ξ_z are the Fermi wave vector

*phong.vo@postgrad.manchester.ac.uk
†niels.walet@manchester.ac.uk
‡francisco.guinea@manchester.ac.uk

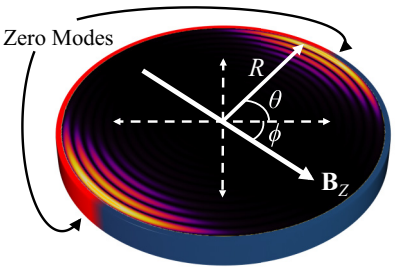

FIG. 1. Schematic representation of a superconducting disk in our setup. An in-plane magnetic field that gives rise to a Zeeman splitting is indicated by the arrow labeled $\mathbf{B}_Z$. The color along the perimeter of the disk indicates relative sign of the superconducting gap at the edge. Majorana zero modes are formed where the gap changes sign, as shown by the bright spots on the disk.

and the penetration length along the z axis. The extraction of an effective low-energy two-dimensional Hamiltonian is described in the Supplemental Material [19]. We obtain

$$\mathcal{H}^{2D}(\mathbf{k}) = E_G\sigma_x + v_F\sigma_z(k_x s_y - k_y s_x), \tag{1}$$

where we denote by σ_i and s_i Pauli matrices that act on orbital space $\{A,B\}$ and spin space $\{\uparrow,\downarrow\}$, respectively, with $i = x,y,z$. We can induce superconductivity in this system via chemical doping. In the mean-field limit, we represent this by a Bogoliubov–de Gennes (BdG) Hamiltonian

$$\mathcal{H}(\mathbf{k}) = [\mathcal{H}^{2D}(\mathbf{k}) - \epsilon_F]\tau_z + \Delta_{sc}\sigma_y s_z \tau_x, \tag{2}$$

where the τ_i are Pauli matrices that act on the Nambu particle-hole space, ϵ_F is the chemical potential, and the coupling $\Delta_{sc}\sigma_y s_z \tau_x$ describes a triplet p-wave, time-reversal-invariant superconductor.

For Bi_2Se_3, and other systems of interest, the chemical potential lies far away from the valence band and the magnitude of the superconducting gap is small, i.e., $\bar{\epsilon}_F = \epsilon_F - E_G \lesssim 2E_G$ and $\Delta_{sc} \ll E_G$. In this limit, we can neglect the valence band, and project the BdG Hamiltonian onto the conduction band only. To lowest order in Δ_{sc}, the Hamiltonian reduces to two 2×2 Hamiltonians $\mathcal{H}_\pm$. Thus, we write the projected Hamiltonian as

$$\mathcal{H}_0(\mathbf{k}) = \begin{pmatrix} \mathcal{H}_+(\mathbf{k}) & 0 \\ 0 & \mathcal{H}_-(\mathbf{k}) \end{pmatrix}, \tag{3}$$

where $\mathcal{H}_\pm(\mathbf{k}) = \pm[\frac{v_F^2|\mathbf{k}|^2}{2E_G} - \bar{\epsilon}_F]\tau_z + \frac{2v_F\Delta_{sc}}{E_G}[k_y\tau_x + k_x\tau_y]$ represents two chiral superconductors with direction-dependent superconducting gaps at the Fermi surface, $\Delta_{sc}^{Fermi} = 2v_F k_F \Delta_{sc} e^{i\varphi}/E_G$, where $\varphi = \arctan(k_y/k_x)$ and $k_F = \sqrt{2E_G\bar{\epsilon}_F}/v_F$. The measured superconducting gap is $2\Delta_{exp} = 2|\Delta_{sc}^{Fermi}| = 4\Delta_{sc}v_F k_F/E_G$. Each chiral superconductor has a single edge mode with a preferred direction [14,34]. The two p-wave branches are related by time-reversal symmetry, making the total Hamiltonian time-reversal invariant. Therefore, when solving for the eigenstates of $\mathcal{H}_0$ we restrict our attention to finding the states of $\mathcal{H}_+$, and determine the eigenstates of $\mathcal{H}_-$ by reversing time (see Fig. 2).

We now study the edge modes on a disk of radius R by diagonalizing $\mathcal{H}_0$ in that domain. In the following, we use dimensionless variables by expressing all energies in units of $\bar{\epsilon}_F$. Then, we can write

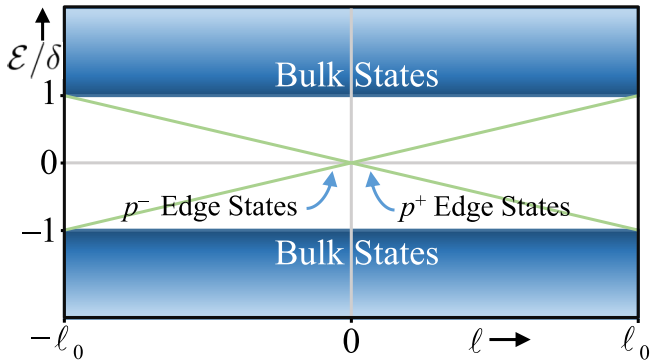

FIG. 2. Schematic of the spectrum of a time-reversal-invariant p-wave superconductor on a disk as a function of angular momentum ℓ. Note that there are two branches of chiral edge modes with opposite chirality below the superconducting gap.

$$\mathcal{H}_\pm(\boldsymbol{\kappa}) = \begin{pmatrix} \pm(|\boldsymbol{\kappa}|^2 - 1) & \sqrt{2\gamma}(-i\kappa_x + \kappa_y) \\ \sqrt{2\gamma}(i\kappa_x + \kappa_y) & \pm(-|\boldsymbol{\kappa}|^2 + 1) \end{pmatrix}, \tag{4}$$

where $\boldsymbol{\kappa} = \mathbf{k}/k_F$, and $\gamma = \Delta_{exp}^2/2\bar{\epsilon}_F^2 \ll 1$ sets the relative scale of the superconducting gap. In our notation, the electron and hole components are ordered as $|\Psi\rangle = (\psi_\uparrow^{(e)} \quad \psi_\downarrow^{(h)} \quad -\psi_\uparrow^{(h)} \quad \psi_\downarrow^{(e)})^T$. The eigenfunctions of the Hamiltonian in Eq. (4) on a disk are two-component spinors, where each component contains the product of radial Bessel functions with wave vector $\kappa = |\boldsymbol{\kappa}|$ and angular momentum ℓ, as discussed in detail in the Supplemental Material [19]. The upper and lower components differ by one unit of angular momentum [35]. We are interested in the case where κ is complex, corresponding to edge modes with an exponentially decaying wave function. This occurs for energies E below the superconducting gap, i.e., $E/\bar{\epsilon}_F = \mathcal{E} < \delta = \Delta_{sc}/\bar{\epsilon}_F$. By imposing the boundary condition that the wave function vanishes on the edge, we can find the energy spectrum for the edge states. In the semiclassical limit where the system size is much larger than the Fermi wavelength $\lambda = k_F R \gg 1$, and to first order in λ^{-1}, the spectra of edge modes for the p^+ and p^- superconductors are

$$\mathcal{E}_\pm^{edge} \approx \mp\left(\ell + \frac{1}{2}\right)\frac{\sqrt{2\gamma}}{\lambda}. \tag{5}$$

We note that Eq. (5) is valid up to $|\ell| \approx \lambda\sqrt{1-\gamma/2}$; for larger angular momenta, the states lie outside the superconducting gap, and they are delocalized. Due to circular symmetry, the probability density of the edge states is uniform along the perimeter of the disk. The decay length towards the interior of the disk is $r_* \propto \xi = \bar{\epsilon}_F/(\Delta_{exp}k_F)$. This length should be smaller than the disk's radius. Table I list estimates of the coherence length and of other parameters. Scalar disorder leads to pair breaking in p-wave superconductors, although the spin-orbit coupling reduces this effect [36]. The parameters in Table I use the critical temperatures taken from experiments [37], which already include the effect of disorder. Finally, it is important to note that scalar disorder does not mix the midgap states.

TABLE I. Relevant parameters, analytical expressions, and numerical estimates of different quantities discussed in the text. Here, k_B is Boltzmann's constant, and μ_e is the magnetic moment of the electron. We estimate these parameters based on experimental data available for $Cu_xBi_2Se_3$ [37,40–44]. Details can be found in the Supplemental Material [19].

Input parameters	Radius	R		1 μm
	Magnetic field	B_Z		1 T
Length and angular scales	Fermi wavelength	k_F		10^{-1} Å^{-1}
	Electron density per layer	ρ_L	$k_F^2/2\pi$	1.6×10^{13} cm^{-2}
	Coherence length	ξ	$0.2\times(\hbar v_F)/(k_B T_c)$	2×10^3 Å
	Angular width of Majorana states	$1/b$	$\sqrt{\Delta_{\rm exp}/(\mu_e B_Z k_F R)}$	0.32 radians
Energy scales	Fermi energy	$\bar{\epsilon}_F$	$v_F^2 k_F^2/2E_G$	$k_B\times2300$ K $=200$ meV
	Critical temperature	T_c		3.8 K
	Superconducting gap	$\Delta_{\rm exp}$	$1.76\,k_B T_c$	$k_B\times6.7$ K $=0.6$ meV
	Quasiparticle gap	Δ_M	$\sqrt{(2\mu_e B_Z \Delta_{\rm exp})/(k_F R)}$	$k_B\times0.3$ K $=0.026$ meV
	Gap between Majorana modes	$\delta\epsilon_M$	$\Delta_M \exp(-2b^2)/\sqrt{2}$	$k_B\times10^{-8}$ K $=10^{-9}$ meV

We now consider a symmetry-breaking perturbation that induces zero-mode Majorana states. We apply an in-plane magnetic field that breaks time-reversal symmetry and induces a superconducting gap that vanishes at boundary points where the field is tangent to the disk. We expect to find localized zero modes at these points. The perturbation is of the form $\mathcal{H}_Z = \tau_Z(\mathcal{E}_Z \mathbf{n}\cdot\mathbf{s})$, where $\mathbf{n}$ points in the direction of the field, $\mathcal{E}_Z = \mu_e B_Z/\bar{\epsilon}_F$ is the Zeeman coupling scaled by $\bar{\epsilon}_F$, and μ_e is the magnetic moment of the electron (see Fig. 1). The Zeeman field couples electrons of opposite spins from the different branches, and likewise, holes from different branches. Note that a parallel magnetic field weakly perturbs the superconducting phase [38,39]. We work in the weak-field limit, where the Zeeman energy is much smaller than the superconducting gap. Then, we can neglect the bulk states, and truncate the Hilbert space to the (unperturbed) edge states only. We project the full Hamiltonian $\mathcal{H} = \mathcal{H}_0 + \mathcal{H}_Z$ onto this basis and diagonalize the truncated Hamiltonian. We find two Majorana zero modes separated in energy from the first excited quasiparticle states by an energy gap Δ_M, which can be expressed as $\Delta_M/\bar{\epsilon}_F \approx (8\gamma/\lambda^2\times\mathcal{E}_Z^2)^{1/4}$ for large λ. This implies stability of the zero-mode states as they are well separated from the other edge modes. A second important scale is the splitting between the two Majorana states. Since the wave function at either side of the disk is approximately Gaussian, with angular width $\langle\theta^2\rangle \approx \sqrt{2\gamma}/(\mathcal{E}_Z\lambda)$, this leads to a splitting which decays exponentially with R. As illustrated here, we can manipulate the gaps that determine the stability of the Majorana modes by simply adjusting the strength of the applied field and the size of the disk.

As the edge modes are localized at boundary points where the superconducting gap changes sign, we can rotate these modes by simply rotating the Zeeman field, as shown Fig. 3. This gives us a simple way to perform particle exchanges for braiding and other purposes. We now explore this possibility in a three-disk configuration. In the presence of tunneling junctions between disks, the Hamiltonian restricted to the Majorana states is

$$\mathcal{H}_M = i\sum_{i,j} t_{i,j}(\phi)\gamma_i\gamma_j, \tag{6}$$

where γ_i and γ_j are Majorana operators in neighboring disks, and $t_{i,j}(\phi)$ is the hopping between those Majorana states. This term depends on the orientation of the field ϕ. By rotating the magnetic field, states in different disks can be brought into contact, as illustrated in Fig. 4. For instance, the change of the exchange field which takes the left configuration into the center one exchanges states 3 and 1, while the change from the center configuration to the right one exchanges states 2 and 6. This scheme shows a simple way to manipulate the Majorana fermions. A complete braiding protocol is outside the scope of this work. An alternative proposal, based on a one-dimensional ring of magnetic atoms on a superconductor,

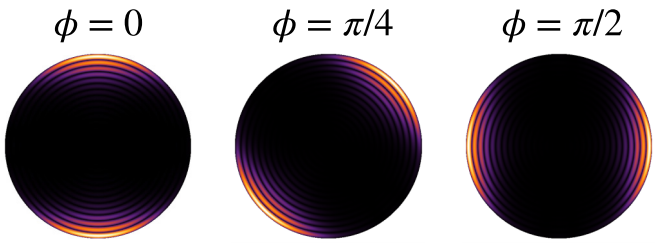

FIG. 3. Majorana zero modes in the presence of a Zeeman field. We plot here the electron densities localized around points where the superconducting gap changes sign. We see that the zero modes rotate as we rotate the in-plane field by changing ϕ. We use the following parameters: $\gamma = \frac{1}{16}$, $\lambda = k_F R = 50$, and $\mathcal{E}_Z = \frac{1}{20}$.

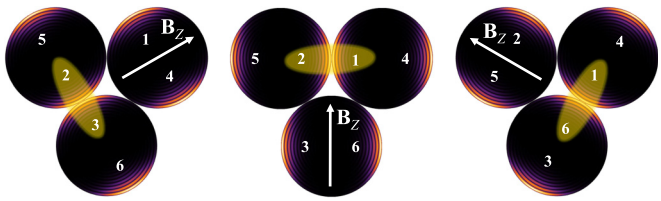

FIG. 4. Manipulation of Majorana modes by an in-plane magnetic field in an array of three topological superconductor quantum dots. The numbers label the Majorana states. Tunneling-assisted mixing between these states occurs when they are in nearby regions of the dots, as shown by the ellipses.

has been recently discussed in [45] (note that the braiding scheme discussed there can be extended to our proposal, using overlapping dots). For other realizations, see also [46,47].

The appeal of this approach is that no trijunctions are required, and only a rotation of the magnetic field is needed. These operations are carried out without recourse to external gates or magnetic fluxes. If such fluxes and gates are added to this system, more ways to correlate the Majorana particles are induced, leading to new functionalities. Furthermore, more complex dot geometries can also be a platform for more ambitious engineering efforts. We explore some of these possibilities in the Supplemental Material [19].

It may also be the case that the magnetic field is due to spontaneously polarized magnetic moments or to an additional chiral superconducting component of the order parameter [22]. Then, quantum fluctuations of the field will lead to additional interactions between the Majorana states. Finally, a large array of quantum dots can serve as a platform for a surface code for topological quantum computation [48–50].

One question that needs to be addressed is whether we can perform the magnetic field rotation without substantially mixing in low-lying fermionic excitations (so-called quasiparticle poisoning [2]). As shown in detail in the Supplemental Material [19], in the limit of weak coupling, we can adjust the separation in energy scales to be large enough to assure that this does not happen. There is a subtle interplay between effective tunneling-supported mixing of the Majorana particles and quasiparticle poisoning that deserves further investigation.

In summary, we have analyzed the emergence of localized Majorana modes at the edges of finite two-dimensional topological superconductors. Although we have based our model on the time-reversal-invariant triplet superconducting phase that is likely to exist in doped Bi_2Se_3, our results apply more generally to systems where the thickness is much smaller than the bulk coherence length. In particular, the triplet superconducting phase of doped Bi_2Se_3 bears qualitative resemblance to the B phase of superfluid ^{3}He, and therefore, we expect our results to hold in that context as well. Furthermore, the analysis remains valid for other gapped superconducting phases with gapless edge modes, such as the nematic phase, also proposed for doped Bi_2Se_3. Similar Majorana states can also be expected in fermionic superfluids based on cold atoms.

Our system provides an appealing alternative Majorana platform precisely because of its simplicity. We can control the stability of the Majorana states by widening the gap to the next excited states with a simple adjustment of the field strength. The positions of the Majorana states can be modified by changing the orientation of the applied magnetic field. Already with a single disk, we can exchange two Majorana particles by rotating the field by π. In arrays with many quantum dots, the field can be used to modulate the interaction between Majorana states in different dots, and to exchange them, without requiring the existence of trijunctions, electrostatic gates, or magnetic fluxes. These properties make the proposed model an interesting candidate for the experimental realization of a Majorana-based qubit for topological quantum computation.

We would like to thank R. Aguado, L. Chirolli, and P. San-Jose for helpful conversations. This work was supported by funding from the European Union through the ERC Advanced Grant NOVGRAPHENE through Grant Agreement No. 290846, and from the European Commission under the Graphene Flagship, Contract No. CNECTICT-604391. V.T.P. acknowledges financial support from the Marshall Aid Commemoration Commission.

[1] C. Beenakker and L. Kouwenhoven, Nat. Phys. **12**, 618 (2016).
[2] S. D. Sarma, M. Freedman, and C. Nayak, NPJ Quantum Inf. **1**, 15001 (2015).
[3] A. Y. Kitaev, Phys. Usp. **44**, 131 (2001).
[4] Y. Oreg, G. Refael, and F. von Oppen, Phys. Rev. Lett. **105**, 177002 (2010).
[5] R. M. Lutchyn, J. D. Sau, and S. Das Sarma, Phys. Rev. Lett. **105**, 077001 (2010).
[6] M. Z. Hasan and C. L. Kane, Rev. Mod. Phys. **82**, 3045 (2010).
[7] X.-L. Qi and S.-C. Zhang, Rev. Mod. Phys. **83**, 1057 (2011).
[8] J. Alicea, Rep. Prog. Phys. **75**, 076501 (2012).
[9] M. Leijnse and K. Flensberg, Semicond. Sci. Technol. **27**, 124003 (2012).
[10] Y. Ando and L. Fu, Annu. Rev. Condens. Matter Phys. **6**, 361 (2015).
[11] D. Aasen, M. Hell, R. V. Mishmash, A. Higginbotham, J. Danon, M. Leijnse, T. S. Jespersen, J. A. Folk, C. M. Marcus, K. Flensberg, and J. Alicea, Phys. Rev. X **6**, 031016 (2016).
[12] C. Kallin and J. Berlinsky, Rep. Prog. Phys. **79**, 054502 (2016).
[13] M. Sato and Y. Ando, Rep. Prog. Phys. **80**, 076501 (2017).
[14] N. Read and D. Green, Phys. Rev. B **61**, 10267 (2000).
[15] P. Fendley, M. P. A. Fisher, and C. Nayak, Phys. Rev. B **75**, 045317 (2007).
[16] J. Alicea, Y. Oreg, G. Refael, F. von Oppen, and M. P. Fisher, Nat. Phys. **7**, 412 (2011).
[17] J. D. Sau, D. J. Clarke, and S. Tewari, Phys. Rev. B **84**, 094505 (2011).
[18] B. van Heck, A. R. Akhmerov, F. Hassler, M. Burrello, and C. W. J. Beenakker, New J. Phys. **14**, 035019 (2012).
[19] See Supplemental Material at http://link.aps.org/supplemental/10.1103/PhysRevB.96.060505 for further details of the calculations and tight-binding calculations in more general geometries.
[20] L. Fu and E. Berg, Phys. Rev. Lett. **105**, 097001 (2010).
[21] J. W. F. Venderbos, V. Kozii, and L. Fu, Phys. Rev. B **94**, 180504 (2016).
[22] L. Chirolli, F. de Juan, and F. Guinea, Phys. Rev. B **95**, 201110 (2017).
[23] L. V. Levitin, R. G. Bennett, A. Casey, B. Cowan, J. Saunders, D. Drung, T. Schurig, and J. M. Parpia, Science **340**, 841 (2013).
[24] L. V. Levitin, R. G. Bennett, A. Casey, B. Cowan, J. Saunders, D. Drung, T. Schurig, J. M. Parpia, B. Ilic, and N. Zhelev, J. Low Temp. Phys. **175**, 667 (2014).
[25] M. Saitoh, H. Ikegami, and K. Kono, Phys. Rev. Lett. **117**, 205302 (2016).
[26] Y. Tsutsumi, M. Ichioka, and K. Machida, Phys. Rev. B **83**, 094510 (2011).

[27] M. J. H. Ku, A. T. Sommer, L. W. Cheuk, and M. W. Zwierlein, Science **335**, 563 (2012).
[28] L. Fu and C. L. Kane, Phys. Rev. Lett. **100**, 096407 (2008).
[29] F. Zhang, C. L. Kane, and E. J. Mele, Phys. Rev. Lett. **111**, 056402 (2013).
[30] A. D. Bernardo, O. Millo, M. Barbone, H. Alpern, Y. Kalcheim, U. Sassi, A. K. Ott, D. D. Fazio, D. Yoon, M. Amado *et al.*, Nat. Commun. **8**, 14024 (2017).
[31] H. Zhang, C.-X. Liu, X.-L. Qi, X. Dai, Z. Fang, and S.-C. Zhang, Nat. Phys. **5**, 438 (2009).
[32] C.-X. Liu, X.-L. Qi, H. J. Zhang, X. Dai, Z. Fang, and S.-C. Zhang, Phys. Rev. B **82**, 045122 (2010).
[33] T. H. Hsieh and L. Fu, Phys. Rev. Lett. **108**, 107005 (2012).
[34] X.-L. Qi, T. L. Hughes, S. Raghu, and S.-C. Zhang, Phys. Rev. Lett. **102**, 187001 (2009).
[35] M. Stone and R. Roy, Phys. Rev. B **69**, 184511 (2004).
[36] K. Michaeli and L. Fu, Phys. Rev. Lett. **109**, 187003 (2012).
[37] Y. S. Hor, A. J. Williams, J. G. Checkelsky, P. Roushan, J. Seo, Q. Xu, H. W. Zandbergen, A. Yazdani, N. P. Ong, and R. J. Cava, Phys. Rev. Lett. **104**, 057001 (2010).
[38] A. M. Clogston, Phys. Rev. Lett. **9**, 266 (1962).
[39] B. S. Chandrasekhar, Appl. Phys. Lett. **1**, 7 (1962).
[40] L. A. Wray, S. Xu, Y. Xia, D. Qian, A. V. Fedorov, H. Lin, A. Bansil, Y. S. Hor, R. J. Cava, and M. Z. Hasan, Nat. Phys. **6**, 855 (2010).
[41] M. Kriener, K. Segawa, Z. Ren, S. Sasaki, S. Wada, S. Kuwabata, and Y. Ando, Phys. Rev. B **84**, 054513 (2011).
[42] G. Zhang, H. Qin, J. Teng, J. Guo, Q. Guo, X. Dai, Z. Fang, and K. Wu, Appl. Phys. Lett. **95**, 053114 (2009).
[43] L. J. Sandilands, A. A. Reijnders, M. Kriener, K. Segawa, S. Sasaki, Y. Ando, and K. S. Burch, Phys. Rev. B **90**, 094503 (2014).
[44] L. A. Wray, S. Xu, Y. Xia, D. Qian, A. V. Fedorov, H. Lin, A. Bansil, L. Fu, Y. S. Hor, R. J. Cava, and M. Z. Hasan, Phys. Rev. B **83**, 224516 (2011).
[45] J. Li, T. Neupert, B. A. Bernevig, and A. Yazdani, Nat. Commun. **7**, 10395 (2016).
[46] S. Nadj-Perge, I. K. Drozdov, B. A. Bernevig, and A. Yazdani, Phys. Rev. B **88**, 020407 (2013).
[47] S. Nadj-Perge, I. K. Drozdov, J. Li, H. Chen, S. Jeon, J. Seo, A. H. MacDonald, B. A. Bernevig, and A. Yazdani, Science **346**, 602 (2014).
[48] S. B. Bravyi and A. Y. Kitaev, arXiv:quant-ph/9811052.
[49] S. Vijay, T. H. Hsieh, and L. Fu, Phys. Rev. X **5**, 041038 (2015).
[50] S. Vijay and L. Fu, Phys. Scr. **T168**, 014002 (2016).